Energy transfer between semiconductor nanocrystals: Validity of Förster's theory

G. Allan and C. Delerue*

*Institut d'Electronique, de Microélectronique et de Nanotechnologie (UMR CNRS 8520), Département ISEN,
41 Boulevard Vauban, F-59046 Lille Cedex, France*
(Received 22 December 2006; revised manuscript received 6 April 2007; published 8 May 2007)

We theoretically study the energy transfer between semiconductor nanocrystals and we calculate the rate of this process in the case of direct-gap (InAs) and indirect-gap (Si) semiconductors. The calculations are based on the tight-binding method that enables us to determine the transfer rate, including electronic structure effects, dielectric screening, and multipolar Coulomb interactions using a microscopic approach. In the case of direct-gap semiconductor nanocrystals, we show that the energy transfer arises only from dipole-dipole interactions in agreement with experimental observations. We obtain that the transfer rate is well described by Förster's theory, and we provide an analytical expression in which the Förster rate is determined not only by the spectral overlap between the emission and absorption spectra of the nanocrystals but also by a factor that simulates the dielectric effects on the Coulomb interactions. In the case of Si nanocrystals, the situation is different because dipolar transitions are weak due to the indirect gap of Si. For this reason, we show that multipolar terms dominate when the distance between the nanocrystals is small and surface effects play an important role in the screening. We predict that the energy transfer between Si nanocrystals by a no-phonon process is possible only when the dots are almost in close contact.

I. INTRODUCTION

Colloidal nanocrystals can be used as building blocks to form molecular[1] or solidlike assemblies such as two-dimensional[2] or three-dimensional colloidal crystals.[3] These systems give the possibility to study the cooperative phenomena that develop when neighbor nanocrystals interact, paving the way to the discovery of materials with new electronic and optical properties.[4] In close-packed assemblies in which there is strong chemical interdot coupling, transport measurements have shown that carriers are mobile by hopping between neighbor nanocrystals.[5,6] When nanocrystals are not chemically coupled, interdot communication remains possible by fluorescence resonant energy transfer[7–11] following Förster's mechanism,[12,13] which is well-known in organic materials. In that case, an exciton created in a nanocrystal (the donor) is transferred to another nanocrystal (the acceptor) with a lower (or equal) energy gap in which radiative recombination can take place. Using this process, tailoring the size of the nanocrystals gives the possibility to engineer energy flows in artificial materials.[9]

All the experiments made so far on the energy transfer between nanocrystals are interpreted using the theory developed by Förster in terms of dipole-dipole interactions,[12,13] theory which was extended by Dexter[14] to include multipole and exchange interactions. In Förster's theory, the dipole in the donor site couples with the absorbing transition in the acceptor one, and the energy transfer rate is given by $\Gamma = (2\pi/\hbar)J^2\Theta$, where J is the dipole-dipole Coulomb coupling and Θ is the overlap between the emission spectrum of the donor chromophore and the absorption spectrum of the acceptor. Γ varies as $1/(R^6\varepsilon_{\text{out}}^2)$, where R is the distance between the two sites and ε_{out} is the dielectric constant of the embedding medium. This theory has been originally developed for molecular systems and has been experimentally confirmed.[15] However, it has never been theoretically validated for nanocrystals, while nanocrystal assemblies are complex dielectric systems in which variations of the fields at the microscopic scale (local fields) play an important role in the optical response.[16,17] Thus, the dipolar approximation and the use of a macroscopic dielectric constant need to be based on a more rigorous basis. In addition, it is not clear whether multipolar interactions become important in closely packed arrays of nanoparticles.[18] There is also a need to perform calculations to predict the energy transfer rates without using experimental inputs. A full treatment implies the calculation of the electronic structure, the Coulomb coupling, and the dielectric screening just starting with the microscopic description of the system.

In this paper, we show that the tight-binding framework is ideally suited to address this complex problem. We present calculations of the energy transfer rate between two nanocrystals. We consider semiconductor materials differing by the nature of their gap, direct (InAs) or indirect (Si). In the case of InAs nanocrystals, we show that the dipolar theory is justified with the rate Γ varying like R^{-6}, but we also show that Γ strongly depends on the dielectric constant of the materials. We study the dependence of the rate on the size of the nanocrystals, and we highlight the importance of the spectral overlap between the excitation spectra of the donor and of the acceptor in agreement with original Förster's theory. We provide a simple expression which, from the knowledge of the emission and absorption spectra, gives the Förster rate taking into account the dielectric environment of the nanocrystals. Thus, one can determine the transfer rate by just calculating the optical properties of the independent nanocrystals. In the case of Si nanocrystals, we show that dipole-dipole interactions only dominate at large distance R, whereas at smaller values, multipole interactions play an important role. This effect is a direct consequence of the weak dipolar transitions in Si nanocrystals due to the indirect gap of the material.[19]
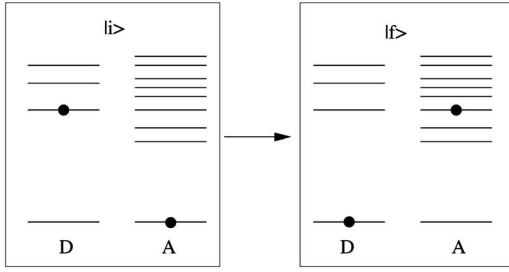
FIG. 1. Many-particle electronic configurations of the donor (D) and acceptor (A) nanocrystals in the (i) initial and (f) final states of the system, before and after the energy transfer.

II. NUMERICAL CALCULATION OF THE TRANSFER RATE

In the following, we consider two nanocrystals (D =donor and A=acceptor) of radius R_D and R_A, respectively. We call R the distance between their centers. An electron-hole pair is created in D, and we study its transfer to A. When R is not too small, the electronic states of the two nanocrystals are nonoverlapping, and they are just coupled by long-range Coulomb interactions. Following the quantum-mechanical derivation of Förster's theory,[13,14] we calculate the energy transfer rate using the Fermi golden rule,

$$\Gamma = \frac{2\pi}{\hbar} \sum_{i,f} p(i) |\langle i|W|f\rangle|^2 \delta(E_i - E_f), \tag{1}$$

where the sum is over the initial ($|i\rangle$) and final ($|f\rangle$) states of energy E_i and E_f, respectively, and $p(i)$ is the thermal population of state $|i\rangle$. W is the screened Coulomb interaction which, due to the inhomogeneous character of the system, must be written as

$$W(\mathbf{r},\mathbf{r}') = \int \varepsilon^{-1}(\mathbf{r},\mathbf{r}'')V(\mathbf{r}'',\mathbf{r}')d\mathbf{r}'', \tag{2}$$

where ε is the static dielectric function and $V(\mathbf{r}'',\mathbf{r}')$ is the bare Coulomb interaction $e^2/|\mathbf{r}''-\mathbf{r}'|$. Thus, the calculation of Γ requires a good description of the electronic states and of the dielectric screening in the system and an evaluation of the matrix elements of the screened potential. We also calculate $\Gamma^{(0)}$ from Eq. (1) in which W is replaced by V to see the effect of the screening on the transfer rate.

The delta function in Eq. (1) means that the total energy is conserved during the transition. To account for the broadening of the levels due to electron-phonon coupling (more generally due to the coupling to the environment), we replace it by a Gaussian of width σ. We take $\sigma=10$ meV, a typical value for nanocrystals in the range of size considered here.[16] More complex line shapes could be introduced to describe the electron-phonon coupling (see, for example, Ref. 7), but it would not change the conclusions of our work.

The initial and final states in Eq. (1) correspond to the many-particle states of the system before and after the energy transfer as depicted in Fig. 1. In the initial states, the donor nanocrystal is in an excited configuration whereas the acceptor one is in its ground state, the situation for the final states being reversed. Working in the strong confinement re-

gime, excitonic effects are neglected, which enables us to define the many-particle states as single Slater determinants built from single-particle states (we will come back to this point later). We assume that, before the energy transfer, the system is in a quasiequilibrium situation, i.e., the electron and the hole in the donor nanocrystal are thermalized in their respective bands and the coefficients $p(i)$ are defined according to a Boltzmann distribution.[19] This approximation is justified when the carrier relaxation is faster than the exciton transfer, which is a likely situation (relaxation lifetimes are typically in the picosecond range[16,20,21]). We denote the single-particle states in the nanocrystal $D(A)$ as $\psi_{n_c}^D$ ($\psi_{n_c}^A$) and $\psi_{n_v}^D$ ($\psi_{n_v}^A$), where c and v represent the empty (conduction) and occupied (valence) states, respectively. Developing the Slater determinants in this basis, Eq. (1) becomes[13,14]

$$\Gamma = \frac{2\pi}{\hbar} \sum_{\substack{n_c,n_v \in D \\ m_c,m_v \in A}} \frac{e^{-(E_{n_c}^D - E_{n_v}^D)/kT}}{Z} |\langle \psi_{n_c}^D \psi_{m_v}^A |W| \psi_{n_v}^D \psi_{m_c}^A \rangle|^2$$

$$\times \delta(E_{n_c}^D - E_{n_v}^D - E_{m_c}^A + E_{m_v}^A), \tag{3}$$

where n_c, n_v, m_c, and m_v include the spin index,

$$Z = \sum_{n_c,n_v \in D} e^{-(E_{n_c}^D - E_{n_v}^D)/kT} \tag{4}$$

and

$$\langle \psi_{n_c}^D \psi_{m_v}^A |W| \psi_{n_v}^D \psi_{m_c}^A \rangle$$
$$= \int \int \psi_{n_c}^{D*}(\mathbf{r}_1) \psi_{m_v}^{A*}(\mathbf{r}_2) W(\mathbf{r}_1,\mathbf{r}_2) \psi_{n_v}^D(\mathbf{r}_1) \psi_{m_c}^A(\mathbf{r}_2) dv_1 dv_2. \tag{5}$$

When the gap of the donor nanocrystal is much larger than the acceptor one, the final states in Eq. (1) correspond to high-energy excitonic states of the acceptor nanocrystal. Thus single-particle energy levels and wave functions must be calculated with a method able to describe them in a wide energy range, which necessitates to go beyond effective mass and $\mathbf{k} \cdot \mathbf{p}$ methods.[16] The tight-binding method provides such a description with a moderate computational cost.[16,19,22–25]

The single-particle wave functions are written in a basis of sp^3 atomic orbitals. The Hamiltonian matrix includes interactions up to third nearest neighbors, providing a very good description of the bulk energy bands for Si (Ref. 22) and InAs.[24] The matrix elements of the screened Coulomb potential $V(\mathbf{r}_1,\mathbf{r}_2)$ are easily calculated because overlaps between atomic orbitals are neglected and because electronic charges localized on the atoms can be approximated by point charges.[16,26,27] The calculation of the dielectric matrix ε and of the screened potential W is described in the Appendix. In the following, we present results obtained for a large number of donor and acceptor sizes. The correlation between confinement energies and size is given in Refs. 22 and 24 for Si and InAs nanocrystals, respectively.

III. ANALYTICAL DERIVATION OF THE TRANSFER RATE

Our main goal in this section is to establish an analytical relation between the transfer rate Γ and two important quantities: first, the overlap between the donor emission spectrum and, the acceptor absorption spectrum, and second, a quantity η describing the dielectric screening in the system and which will only depend on the nature of the materials and on geometrical factors. Thus, we assume that we can replace W by ηV in Eq. (1).

A. Definition of the Förster rate and of the spectral overlap

We must calculate the matrix elements of the Coulomb interaction $V = e^2/|\mathbf{R} + \mathbf{r}_D - \mathbf{r}_A|$ between two electrons in the donor and the acceptor, respectively. $\mathbf{R}$ is the vector joining the nanocrystal centers and $\mathbf{r}_D$ ($\mathbf{r}_A$) is the vector position measured from the center of the donor (acceptor). Following Ref. 14, we expand V in a Taylor series about $\mathbf{R}$ and we only keep the first nonzero contribution,

$$V_{\text{dip}} = (e^2/R^3)\{\mathbf{r}_D \cdot \mathbf{r}_A - 3(\mathbf{r}_D \cdot \mathbf{R})(\mathbf{r}_A \cdot \mathbf{R})/R^2\}, \quad (6)$$

corresponding to the dipole-dipole interaction. The injection of Eq. (6) into Eq. (3) leads to an expression which includes matrix elements $\langle \psi^D_{n_c} | \mathbf{r}_D | \psi^D_{n_v} \rangle$ and $\langle \psi^A_{m_c} | \mathbf{r}_A | \psi^A_{m_v} \rangle$. Because the nanocrystals have almost a spherical symmetry, we can replace the absolute square of the matrix elements in Eq. (3) by their average over all possible orientations of $\mathbf{R}$.[28] Following Ref. 14, the average is

$$\langle |\langle \psi^D_{n_c} \psi^A_{m_v} | V_{\text{dip}} | \psi^D_{n_v} \psi^A_{m_c} \rangle|^2 \rangle_{\text{av}} = \frac{2e^4}{3R^6} |\langle \mathbf{r}^D_{n_c n_v} \rangle|^2 |\langle \mathbf{r}^A_{m_c m_v} \rangle|^2, \quad (7)$$

where

$$|\langle \mathbf{r}^D_{n_c n_v} \rangle|^2 = |\langle \psi^D_{n_c} | x_D | \psi^D_{n_v} \rangle|^2 + |\langle \psi^D_{n_c} | y_D | \psi^D_{n_v} \rangle|^2 + |\langle \psi^D_{n_c} | z_D | \psi^D_{n_v} \rangle|^2. \quad (8)$$

From Eq. (3), we deduce the transfer rate Γ_F following Förster's theory,

$$\Gamma_F = \frac{4\pi}{3\hbar} \frac{e^4 \eta^2}{R^6} \sum_{\substack{n_c, n_v \in D \\ m_c, m_v \in A}} \frac{e^{-(E^D_{n_c} - E^D_{n_v})/kT}}{Z} |\langle \mathbf{r}^D_{n_c n_v} \rangle|^2 |\langle \mathbf{r}^A_{m_c m_v} \rangle|^2$$

$$\times \delta(E^D_{n_c} - E^D_{n_v} - E^A_{m_c} + E^A_{m_v}). \quad (9)$$

The lifetime $\tau_{n_c n_v}$ for the spontaneous radiative transition of an electron in the donor from the state $\psi^D_{n_c}$ to the state $\psi^D_{n_v}$ is given by[14,29]

$$\frac{1}{\tau_{n_c n_v}} = \frac{4e^2 (E^D_{n_c} - E^D_{n_v})^3}{3c^3 \hbar^4} |\langle \mathbf{r}^D_{n_c n_v} \rangle|^2. \quad (10)$$

It is important to note that this definition of the spontaneous lifetime holds for the emission of a photon in vacuum and does not include local-field effects.[14] We will come back to these points later. Then, we can define the emission spectrum of the donor nanocrystal as

$$L(\hbar\omega) = \sum_{n_c, n_v \in D} \frac{e^{-(E^D_{n_c} - E^D_{n_v})/kT}}{Z \tau_{n_c n_v}} \delta(\hbar\omega - E^D_{n_c} + E^D_{n_v}), \quad (11)$$

where $\hbar\omega$ is the photon energy. $L(\hbar\omega)$ provides the shape of the emission spectrum, and its integral $\int L(\hbar\omega) d\hbar\omega$ is equal to the average decay probability, $1/\bar{\tau}$.

We define the absorption cross section of the acceptor nanocrystal as[16]

$$\sigma(\hbar\omega) = \sum_{m_c, m_v \in A} \frac{4\pi^2 \omega e^2}{c} \frac{|\langle \mathbf{r}^A_{m_c m_v} \rangle|^2}{3} \delta(\hbar\omega - E^A_{m_c} + E^A_{m_v}). \quad (12)$$

Equivalently, we can define the optical absorption coefficient $\alpha(\hbar\omega) = \sigma(\hbar\omega)/\Omega_A$, where Ω_A is the volume of the nanocrystal. Once again, these definitions do not include local-field factors and, thus, cannot be compared directly to experiments. Using Eqs. (9)–(12), we deduce a final expression of the Förster transfer rate as

$$\Gamma_F = \frac{3\eta^2 c^4}{4\pi R^6} \int \frac{L(\hbar\omega)\sigma(\hbar\omega)}{\omega^4} d(\hbar\omega), \quad (13)$$

which, in the common situation where the luminescence spectrum can be replaced by a delta function at the energy $\hbar\omega$, becomes

$$\Gamma_F \approx \frac{3\eta^2 c^4}{4\pi R^6} \frac{\sigma(\hbar\omega)}{\bar{\tau}\omega^4}. \quad (14)$$

B. Definition of the screening factor η

We discuss in the following how it is possible to describe the effect of the screening on the electron-electron interaction through a simple factor η. The basic idea is to consider the screening of the dipole-dipole interaction between two nanocrystals using classical electrostatics. It was shown that the dielectric response of nanocrystals differs from the bulk one because it is strongly reduced near the surfaces while it is bulklike inside the nanocrystal.[27,30,31] However, for some properties, it is still possible to define effective values which correspond to averages over the nanocrystal volume and which decrease at decreasing nanocrystal size.[27,30,32] Although approximate, this approach enables us to get a compact expression for the dielectric screening in nanoscale materials. Thus, we assume that the donor and acceptor nanocrystals can be described by dielectric constants $\varepsilon^D_{\text{in}}$ and $\varepsilon^A_{\text{in}}$, respectively. Their size dependence is written as

$$\varepsilon^{D(A)}_{\text{in}} = 1 + (\varepsilon^{\text{bulk}}_{\text{in}} - 1)(1 - \delta/R_{D(A)}), \quad (15)$$

where δ is of the order of the Thomas-Fermi wavelengths.[30,33] In addition, we consider that the two nanocrystals are embedded in a dielectric material of dielectric constant ε_{out}.

To calculate the dipole-dipole interaction, we consider a dipole situated at the center of D and we calculate the electrostatic potential $\phi_{\text{out}}(\mathbf{r})$ outside the dot ($r > R_D$). Opposite charges $+q$ and $-q$ are positioned at $\mathbf{s}$ and $-\mathbf{s}$, respectively

($s=|\mathbf{s}|<R_D$). The dipole is $\mathbf{p}=2q\mathbf{s}$, and $\phi_{\text{out}}(\mathbf{r})$ is given by[34]

$$\phi_{\text{out}}(\mathbf{r}) = \zeta(\mathbf{r},\mathbf{s}) - \zeta(\mathbf{r},-\mathbf{s}), \qquad (16)$$

where

$$\zeta(\mathbf{r},\mathbf{s}) = \frac{q}{\varepsilon_{\text{in}}^D |\mathbf{r} - \mathbf{s}|} \qquad (17)$$

$$+ q\left(1 - \frac{\varepsilon_{\text{out}}}{\varepsilon_{\text{in}}^D}\right)\sum_{l=0}^{\infty} \frac{s^l(l+1)P_l(\cos(\theta))}{[\varepsilon_{\text{in}}^D l + \varepsilon_{\text{out}}(l+1)]r^{l+1}}. \qquad (18)$$

θ is the angle between the vectors $\mathbf{r}$ and $\mathbf{s}$, and P_n is the nth Legendre polynomial. If we keep only the dipolar term, we obtain

$$\phi_{\text{out}}(\mathbf{r}) \approx \left(\frac{3}{\varepsilon_{\text{in}}^D + 2\varepsilon_{\text{out}}}\right)\phi_{\text{dip}}(\mathbf{r}), \qquad (19)$$

where $\phi_{\text{dip}}(\mathbf{r})=p\cos(\theta)/r^2$ is the potential induced by the dipole in vacuum. The same relation holds between the respective electric fields $\mathbf{E}_{\text{out}}$ and $\mathbf{E}_{\text{dip}}$. To calculate the electric field $\mathbf{E}_{\text{in}}^A$ in A due to the dipole in D, we must take into account the effect of the dielectric screening in A. We simply write $\mathbf{E}_{\text{in}}^A \approx 3\varepsilon_{\text{out}}/(\varepsilon_{\text{in}}^A+2\varepsilon_{\text{out}})\mathbf{E}_{\text{out}}$, an expression which normally holds for the electric field inside a dielectric sphere in response to a homogeneous electric field.[16,34] Combining these equations, we obtain $\mathbf{E}_{\text{in}}^A = \eta\mathbf{E}_{\text{dip}}$, where $\mathbf{E}_{\text{dip}}$ is the electric field of the dipole in vacuum and

$$\eta \approx \frac{3\varepsilon_{\text{out}}}{(\varepsilon_{\text{in}}^D + 2\varepsilon_{\text{out}})(\varepsilon_{\text{in}}^A + 2\varepsilon_{\text{out}})}. \qquad (20)$$

This derivation of η is clearly approximate, since, in particular, it neglects the mutual influence between A and D. However, we will see that Eq. (20) provides a reasonable description of the screening of dipole-dipole interactions between two quantum dots. Furthermore, it is exact in two limits, when $\varepsilon_{\text{in}}^D = \varepsilon_{\text{in}}^A = \varepsilon_{\text{out}}$ and when $R \rightarrow \infty$.

IV. InAs QUANTUM DOTS: RESULTS AND DISCUSSIONS

A. Dependence of the transfer rate on the distance between nanocrystals

Figure 2 presents the variation of the transfer time $(1/\Gamma, 1/\Gamma^{(0)})$ with respect to the distance R between two identical InAs nanocrystals. Similar results are obtained for nanocrystals of different sizes. Γ varies almost exactly like R^{-6} in a wide range of distance, showing that the transition is induced by dipole-dipole interactions even when the two nanocrystals are almost in contact. Multipolar interactions are not involved in the transition. Thus, our work confirms the conclusions of Kagan *et al.*[7] that the energy transfer in assemblies of nanocrystals arises from dipole-dipole interdot interactions. As shown by the large difference between Γ and $\Gamma^{(0)}$, the dielectric screening has a strong influence on the energy transfer rate but it does not affect the R^{-6} law. Consequently, the ratio between $\Gamma^{(0)}$ and Γ does not depend on R.
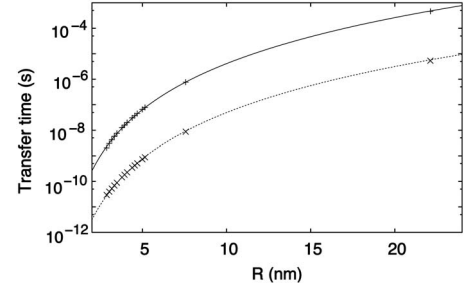

FIG. 2. Energy transfer time ($+$, $1/\Gamma$; $\times$, $1/\Gamma^{(0)}$) between two identical InAs nanocrystals (radius=1.52 nm) in vacuum versus the interdot distance R. Γ is calculated using the screened Coulomb interaction, and $\Gamma^{(0)}$ using the bare one. The solid (dotted) curve shows that $1/\Gamma$ ($1/\Gamma^{(0)}$) varies like R^6.

B. Screening factor

By definition, $\Gamma/\Gamma^{(0)}$ describes the effect of the screening on the energy transfer rate. Figure 3 shows that, in average, $\Gamma/\Gamma^{(0)}$ is close to η^2, where η is given by Eqs. (15) and (20). Thus, η^2 provides a simple expression for the dependence of the rate on the effective dielectric constant of the materials. However, the dispersion of $\Gamma/\Gamma^{(0)}$ with respect to η^2 is not negligible due to the approximations used to derive Eq. (20) and due to the fact that the effective dielectric constant is just an average notion.[16,27,30] Main differences with respect to the average values are due to microscopic effects on the dielectric response and, thus, can only be calculated using a microscopic approach.

C. Comparison with Förster's theory

Figure 4 presents the transfer time between two InAs nanocrystals in various situations ($R=10$ nm) and compares the results of the full calculation with those obtained using the Förster's theory [Eq. (13)]. The agreement between the two calculations is excellent over many orders of magnitude. Similar agreement is obtained for other values of R. We have checked that the discrepancies between the two results only
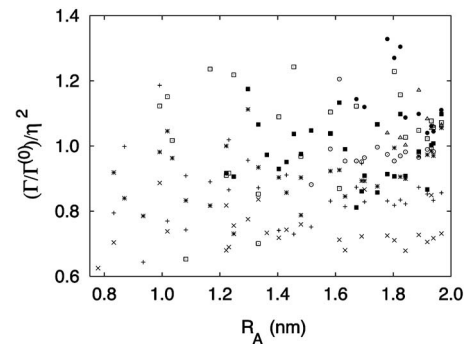

FIG. 3. Ratio $(\Gamma/\Gamma^{(0)})/\eta^2$ calculated for InAs nanocrystals in vacuum versus the radius R_A of the acceptor. The figure shows that $\Gamma/\Gamma^{(0)}$ is close to η^2, in average. The radii of the donors are 0.58 nm ($+$), 0.68 nm ($\times$), 0.83 nm ($*$), 0.99 nm ($\square$), 1.22 nm ($\blacksquare$), 1.52 nm ($\odot$), 1.67 nm ($\bullet$), and 1.82 nm ($\triangle$). η is calculated from Eqs. (15) and (20) using $\delta=0.324$ nm, $\varepsilon_{\text{out}}=1$, and $\varepsilon_{\text{in}}^{\text{bulk}}=9.21$.
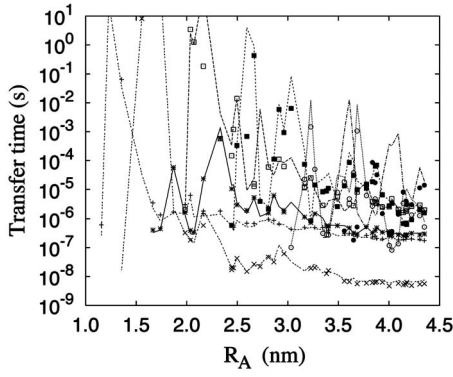
FIG. 4. Calculated energy transfer time $1/\Gamma$ for InAs nanocrystals in vacuum plotted versus the radius R_A of the acceptor (interdot distance $R=10$ nm). The radii of the donors are 0.58 nm (+), 0.68 nm ($\times$), 0.83 nm (*), 0.99 nm ($\square$), 1.22 nm (■), 1.52 nm (○), 1.67 nm (•), 1.82 nm (△). The lines connect the values $1/\Gamma_F$ calculated for the same nanocrystal sizes using Eq. (13) based on Förster's theory ($\varepsilon_{out}=1$).

come from the approximations used to define the screening factor η (the agreement is almost perfect when we compare the lifetimes calculated with the unscreened Coulomb interaction). The large fluctuations of the transfer time $1/\Gamma$ in Fig. 4 are a consequence of the discrete character of the density of states in the acceptor nanocrystal due to the quantum confinement. The energy transfer is only possible when there is a good overlap between the emission spectrum of the donor and the absorption spectrum of the acceptor. The same effect of the overlap appears in Γ_F [Eq. (13)], explaining why Γ and Γ_F capture the same fluctuations. For the same reason, the comparison between Γ and Γ_F remains excellent independently of the width σ of the Gaussians that we take to broaden the delta functions in both calculations.

Thus, we conclude that Γ_F in Eq. (13) provides a simple expression of the transfer rate between two direct-gap semiconductor nanocrystals, since it only requires the calculation of the luminescence and absorption spectra of the respective nanocrystals, which is a much simpler task than to evaluate Γ directly from Eq. (3). In addition, from Eq. (13), it becomes easier to take into account more complex phenomena which may be involved in the energy transfer, such as excitonic effects or more complex line shapes due to the electron-phonon interaction. Dynamical effects could be also included, replacing in Eqs. (13) and (20) the static dielectric constant by its value calculated at the transition energy.

D. Determination of the energy transfer rate from experimental quantities

The luminescence and absorption spectra of the respective nanocrystals can be measured experimentally and, thus, can be used to estimate the energy transfer rate Γ. However, it must be done with some care because Γ depends not only on the intrinsic properties of the nanocrystals but also on the dielectric properties of the surrounding materials. Let us consider a typical situation. One measures the luminescence spectrum $L_{exp}(\hbar\omega)$ and the absorption cross section $\sigma_{exp}(\hbar\omega)$
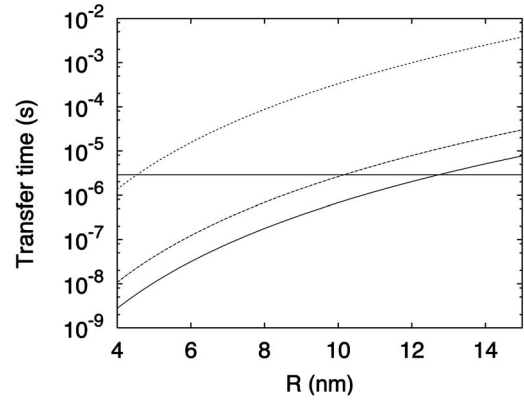

FIG. 5. Lifetime for the energy transfer between two InAs nanocrystals (radius of the donor=1.22 nm) in vacuum versus the interdot distance R. Radii of the acceptors: 2.07 nm (solid curve), 1.75 nm (dashed curve), and 1.25 nm (dotted curve). The horizontal line denotes the radiative lifetime τ_{exp} of the donor in vacuum.

of the nanocrystals diluted in a material of dielectric constant ε_{out}. These quantities differ from those defined in Eqs. (11) and (12) due to local-field factors. For nanocrystals of dielectric constant ε_{in}, and in the limit where the nanocrystals represent a small volume fraction of the medium, we can write[16]

$$L_{exp}(\hbar\omega) = F^2 n L(\hbar\omega),$$

$$\sigma_{exp}(\hbar\omega) = F^2 \sigma(\hbar\omega)/n, \qquad (21)$$

where $F=3\varepsilon_{out}/(\varepsilon_{in}+2\varepsilon_{out})$ is the local-field factor and n is the refractive index of the medium ($\approx\sqrt{\varepsilon_{out}}$). Similarly, the measured radiative lifetime τ_{exp} of the nanocrystals is given by[16]

$$\tau_{exp} = \overline{\tau}/(F^2 n). \qquad (22)$$

Thus, from the experimental optical properties of the nanocrystals, we can deduce $L(\hbar\omega)$, $\sigma(\hbar\omega)$, and $\overline{\tau}$, from which we can estimate Γ_F from Eqs. (13) and (14). However, we must pay attention to the fact that the evaluation of Eqs. (13) and (14) requires, in principle, us to know the quantities corresponding to single quantum dots whereas most of the time measurements are made on ensembles of dots.

E. Energy transfer versus radiative recombination

We discuss now the respective efficiency of the energy transfer and of the radiative recombination of the exciton in the donor. We consider a donor nanocrystal in vacuum, and Fig. 5 compares its radiative lifetime τ_{exp} [Eq. (22)] with the transfer time calculated for three acceptor sizes. We obtain that the energy transfer is more efficient than the radiative recombination when $R \lesssim 10-12$ nm for the largest acceptor nanocrystals, in agreement with the experiments on direct-gap semiconductor nanocrystal assemblies.[7–11]

Figure 5 shows that the radiative lifetime that we calculate is long ($\tau_{exp}=0.3$ μs) because the optical transition from the lowest unoccupied state (denoted $1S_e$ in Ref. 24) to the highest occupied state (1_H) has a very small oscillator strength. The first optically allowed transition takes place
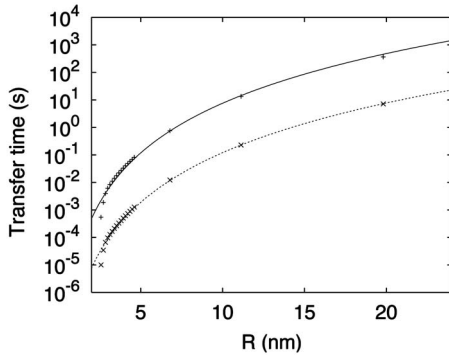
FIG. 6. Energy transfer time ($+$, $1/\Gamma$; $\times$, $1/\Gamma^{(0)}$) between two identical Si nanocrystals (radius=1.36 nm) in vacuum versus the interdot distance R. Γ is calculated using the screened Coulomb interaction, and $\Gamma^{(0)}$ using the bare one. The solid (dotted) curve shows that $1/\Gamma$ ($1/\Gamma^{(0)}$) varies like R^6 at large distance.

FIG. 7. Energy transfer time $1/\Gamma$ calculated for Si nanocrystals in vacuum and plotted versus the radius R_A of the acceptor (interdot distance $R=10$ nm). Radii of the donors: 0.52 nm ($\times$), 0.61 nm ($+$), 0.75 nm ($*$), 0.84 nm ($\square$), 1.09 nm ($\blacksquare$), 1.36 nm ($\odot$), 1.50 nm ($\bullet$), and 1.63 nm ($\triangle$).

with the second occupied state (2_H) which is only 114 meV below 1_H. These selection rules are due to the spherical shape of the nanocrystal ($\approx T_d$ symmetry) and the $1S_e$, 1_H, and 2_H states have a symmetry close to A_1, T_1, and T_2, respectively ($A_1 \rightarrow T_1$ is forbidden, $A_1 \rightarrow T_2$ is allowed). In the case of a nanocrystal with a less symmetric shape, the T_1 and T_2 states are mixed, the lowest optical transition becomes allowed, and the radiative lifetime reaches values in the 10 ns range. However, in that case, because the transfer rate is proportional to the radiative recombination rate, all the curves in Fig. 5 would be shifted in the same way, and the conclusions on the respective efficiency of the two processes would remain the same.

V. Si QUANTUM DOTS: RESULTS AND DISCUSSIONS

A. Dependence of the transfer rate on the distance between nanocrystals

The situation for Si nanocrystals is more complex because it is an indirect-gap semiconductor. The first difference with InAs can be seen in Fig. 6, where we plot $1/\Gamma$ and $1/\Gamma^{(0)}$ as functions of the interdot distance R. The R^6 dependence is found except when R is small, of the order of the nanocrystal radius, where the transfer times vary much faster with R. In this limit, multipolar interactions become larger than dipolar ones, and this effect is a consequence of the indirect nature of the Si band gap. In the bulk, the direct radiative recombination of electron-hole pairs is forbidden and the recombination is only possible with the assistance of phonons. In nanocrystals, direct no-phonon transitions become slightly allowed due to the fact that a confinement in real space leads to a spread of the wave functions in **k** space.[16,35,36] Thus, each optical matrix element is a function of the overlap in **k** space between the electron and hole wave functions. This overlap is extremely small and the lifetime is long (basically in the millisecond to microsecond range). Consequently, at decreasing interdot distance, multipolar terms increase faster than dipolar ones and, thus, become more important below a threshold of the order of the nanocrystal size.

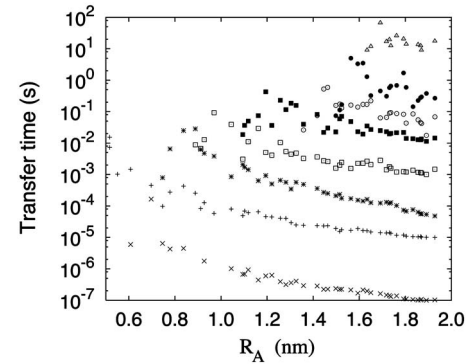The difference with InAs is also visible in Fig. 7 showing

the dependence of the transfer time $1/\Gamma$ on the size of the nanocrystals when R is large (10 nm), i.e., when dipolar terms dominate. When the size of the donor nanocrystal increases, the transfer time increases by orders of magnitude because the dipolar recombination rate vanishes (in comparison, the distribution of $1/\Gamma$ is much smaller for InAs, see Fig. 4). A similar evolution is obtained for the radiative lifetime as a function of the nanocrystal size.[16,35,36] There is also a smaller variation of $1/\Gamma$ with the radius of the acceptor: $1/\Gamma$ decreases at increasing R_A due to an enhanced optical absorption at a fixed energy when going to larger sizes.

B. Screening factor and comparison with Förster's theory

By comparison with the full calculation, we have obtained that Eq. (13) corresponding to Förster's theory cannot be used to calculate the transfer rate for Si nanocrystals, not only at small values of R when multipolar terms dominate but also at larger values. At large R, the problem comes from the screening factor, and not from the spectral overlap. Figure 8 shows that $1/\Gamma^{(0)}$ is almost perfectly given by Eq. (13) with $\eta=1$ [$1/\Gamma^{(0)} \approx 1/\Gamma_F^{(0)}$ when $R \gg R_A, R_D$]. The transfer rate calculated with the unscreened Coulomb interaction is entirely described by the overlap between the emission spectrum of the donor and the absorption spectrum of the acceptor. However, the ratio $\Gamma/\Gamma^{(0)}$ cannot be described by the factor η^2 like in the case of InAs. The indirect character of the Si band gap is once again at the origin of this difference. In contrast to the bulk, the dipolar terms are not equal to zero in Si nanocrystals because of the confinement. Thus, the optical matrix elements only contain contributions coming from the atoms near the surfaces where the electric field is less screened than inside the nanocrystals. Therefore, the screening factor cannot be approximated by Eq. (20) and must be calculated using a microscopic approach. However, for practical purposes, Figs. 7 and 8 already provide the transfer time in two opposite situations, when $\varepsilon_{out}=1$ (Fig. 7) and when $\varepsilon_{out}=\varepsilon_{in}^{bulk}$ (Fig. 8 using the fact that we have just to multiply $1/\Gamma^{(0)}$ by $\{\varepsilon_{in}^{bulk}\}^2$).
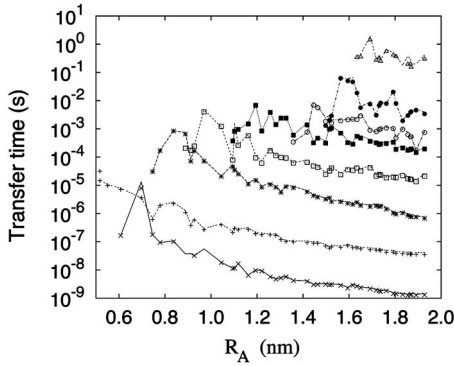
FIG. 8. Energy transfer time $1/\Gamma^{(0)}$ calculated using the unscreened Coulomb interaction for Si nanocrystals in vacuum and plotted versus the radius R_A of the acceptor (interdot distance R =10 nm). Radii of the donors: 0.52 nm ($\times$), 0.61 nm ($+$), 0.75 nm ($*$), 0.84 nm ($\square$), 1.09 nm ($\blacksquare$), 1.36 nm ($\bigcirc$), 1.50 nm ($\bullet$), and 1.63 nm ($\triangle$). The lines connect the values $1/\Gamma_F^{(0)}$ calculated for the same nanocrystal sizes using Eq. (13) with η=1.

C. Energy transfer versus radiative recombination

We have already confirmed that the energy transfer between two nanocrystals can be more efficient than the radiative recombination in the case of direct-gap semiconductors, as observed experimentally.[7–11] In the case of Si nanocrystals, the situation is once again different. Figure 9 compares the transfer lifetime and the radiative lifetime in typical situations. It shows that energy transfer is possible but only when the two Si nanocrystals are almost in contact. However, we have considered here no-phonon processes, and it is likely that phonon-assisted processes are also involved in the energy transfer such as in the radiative recombination. The calculation of the transfer rate including these processes is obviously a difficult task and beyond the scope of the present paper.

VI. CONCLUSION

The energy transfer between semiconductor nanocrystals is a phenomenon of growing interest to engineer energy
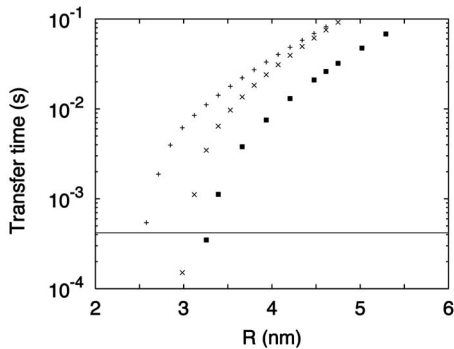

FIG. 9. Lifetime for the energy transfer between two Si nanocrystals (diameter of the donor=2.7 nm) in vacuum versus the interdot distance R. Diameters of the acceptors: 2.7 nm ($+$), 3.3 nm ($\times$), and 3.9 nm ($\blacksquare$). The horizontal line denotes the radiative lifetime $\tau_{\exp}$ of the donor in vacuum.

flows in artificial materials.[9] Its description is usually based on Förster's theory in terms of dipole-dipole interactions. In this work, we present theoretical calculations of the energy transfer rate which fully justify the application of Förster's theory in the case of direct-gap semiconductor nanocrystals. We show that the multipole interactions are negligible even when the distance between the nanocrystals is small. We provide an analytical formula to calculate the Förster rate using the emission spectrum, the absorption cross section, and the effective dielectric constant of the nanocrystals. In the case of Si nanocrystals, we show that multipolar interactions are important at short interdot distances and that dipole-dipole interactions dominate otherwise. We conclude that Förster's theory cannot be applied to the no-phonon process of energy transfer between indirect-gap semiconductor nanocrystals.

APPENDIX: CALCULATION OF THE SCREENED COULOMB POTENTIAL

Here, we describe the calculation of the Coulomb potential $V(\mathbf{r},\mathbf{r}')$, of the dielectric constant $\varepsilon(\mathbf{r},\mathbf{r}')$, and of the screened potential $W(\mathbf{r},\mathbf{r}')$ in tight binding. As discussed in Refs. 16 and 27, tight binding leads to a considerable simplification because the functions of $\mathbf{r}$ are evaluated at discrete values corresponding to the atomic positions $\mathbf{R}_n$ and because the overlaps between atomic wave functions are neglected. Thus, V, ε, and W are described by matrices whose size is given by the number of atoms in the system. The matrix of the bare Coulomb potential V is given by[26]

$$V_{nm} = e^2/|\mathbf{R}_n - \mathbf{R}_m| \quad \text{if } n \neq m,$$

$$V_{nn} = U_n^{\text{at}}, \tag{A1}$$

where U_n^{at} is the intraatomic Coulomb energy on the atom n.

The dielectric response is calculated in the random-phase approximation (or linearized time-dependent Hartree)[16,37] leading to $\varepsilon = I - V\chi$ and $W = \varepsilon^{-1}V$. χ is the matrix of the noninteracting density response function (polarization) given by

$$\chi_{nm} = \sum_{n_c,n_v} \left[\sum_\alpha a_{n_c,m\alpha} a_{n_v,m\alpha}^* \right] \left[\sum_\alpha a_{n_v,n\alpha} a_{n_c,n\alpha}^* \right]$$
$$\times \left\{ \frac{1}{E_{n_v} - E_{n_c} - i0^+} - \frac{1}{E_{n_c} - E_{n_v} - i0^+} \right\} \tag{A2}$$

when the one-electron wave functions are defined by $\psi_{n_c} = \sum_{n\alpha} a_{n_c,n\alpha} \phi_{n\alpha}$ in the basis of atomic orbitals $\{\phi_{n\alpha}\}$, where n denotes the atomic site and α the atomic orbital (similar definition holds for ψ_{n_v}). The coefficients $a_{n_c,n\alpha}$ are obtained by the diagonalization of the tight-binding Hamiltonian, and, thus, the calculation of ε and W is straightforward. However, the calculation of χ becomes prohibitive for nanocrystals containing a large number of atoms due to the double sum in Eq. (A2). Thus, we have used an approximation which considerably reduces the computational cost. We have calculated the density response function χ^{bulk} of the bulk semiconductors, and we have transferred its components to the case of nanocrystals using the fact that the quantum confinement

plays no role in the static dielectric response of nanocrystals.[30,31] We write

$$\chi_{nm} = \chi_{nm}^{\text{bulk}} \quad \text{if } n \neq m, \tag{A3}$$

$$\chi_{nn} = -\sum_{m \neq n} \chi_{nm}^{\text{bulk}}. \tag{A4}$$

Equation (A3) is justified by Fig. 6 of Ref. 30 showing that χ_{nm} (denoted by P in this paper) does not depend on the nanocrystal size and, thus, can be replaced by its bulk value. Equation (A4) is derived from the sum rules $\Sigma_m \chi_{nm} = 0$, $\forall n$, which state that the total charge is conserved in the system in response to a constant perturbation. We have checked that this approximation works very well compared to the full calculation, for example, when looking at the response of the nanocrystal to a homogeneous electric field.

---

*Electronic address: christophe.delerue@isen.fr

[1] R. Koole, P. Liljeroth, C. de Mello Donegá, D. Vanmaekelbergh, and A. Meijerink, J. Am. Chem. Soc. **128**, 10436 (2006).

[2] D. Battaglia, J. L. Li, Y. Wang, and X. Peng, Angew. Chem., Int. Ed. **42**, 5035 (2003).

[3] A. L. Rogach, D. V. Talapin, E. V. Shevchenko, A. Kornowski, M. Haase, and H. Weller, Adv. Funct. Mater. **12**, 653 (2002).

[4] C. B. Murray, C. R. Kagan, and M. G. Bawendi, Science **270**, 1335 (1995).

[5] A. L. Roest, J. J. Kelly, D. Vanmaekelbergh, and E. A. Meulenkamp, Phys. Rev. Lett. **89**, 036801 (2002).

[6] D. Yu, C. Wang, and P. Guyot-Sionnest, Science **300**, 1277 (2003).

[7] C. R. Kagan, C. B. Murray, and M. G. Bawendi, Phys. Rev. B **54**, 8633 (1996).

[8] O. I. Micic, K. M. Jones, A. Cahill, and A. J. Nozik, J. Phys. Chem. B **102**, 9791 (1998).

[9] S. A. Crooker, J. A. Hollingsworth, S. Tretiak, and V. I. Klimov, Phys. Rev. Lett. **89**, 186802 (2002).

[10] T. Franzl, D. S. Koktysh, T. A. Klar, A. L. Rogach, J. Feldmann, and N. Gaponik, Appl. Phys. Lett. **84**, 2904 (2004).

[11] T. Pons, I. L. Medintz, M. Sykora, and H. Mattoussi, Phys. Rev. B **73**, 245302 (2006).

[12] T. Förster, Naturwiss. **33**, 166 (1946); Ann. Phys. **2**, 55 (1948).

[13] R. M. Clegg, in *Fluorescence Imaging Spectroscopy and Microscopy*, edited by Xue Fen Wang and Brian Herman, Chemical Analysis Series Vol. 137 (Wiley-Interscience, New York, 1996), p. 179.

[14] D. L. Dexter, J. Chem. Phys. **21**, 836 (1953).

[15] A. A. Deniz, M. Dahan, J. R. Grunwell, T. Ha, A. E. Faulhaber, D. S. Chemla, S. Weiss, and P. G. Schultz, Proc. Natl. Acad. Sci. U.S.A. **96**, 3670 (1999).

[16] C. Delerue and M. Lannoo, *Nanostructures: Theory and Modelling* (Springer-Verlag, Berlin, 2004).

[17] F. Trani, D. Ninno, G. Cantele, G. Iadonisi, K. Hameeuw, E. Degoli, and S. Ossicini, Phys. Rev. B **73**, 245430 (2006).

[18] R. Rojas and F. Claro, Phys. Rev. B **34**, 3730 (1986).

[19] C. Delerue, G. Allan, and M. Lannoo, Phys. Rev. B **48**, 11024 (1993).

[20] R. D. Schaller, J. M. Pietryga, S. V. Goupalov, M. A. Petruska, S.

A. Ivanov, and V. I. Klimov, Phys. Rev. Lett. **95**, 196401 (2005).

[21] B. L. Wehrenberg, C. Wang, and P. Guyot-Sionnest, J. Phys. Chem. B **106**, 10634 (2002).

[22] Y. M. Niquet, C. Delerue, G. Allan, and M. Lannoo, Phys. Rev. B **62**, 5109 (2000).

[23] G. Allan, Y. M. Niquet, and C. Delerue, Appl. Phys. Lett. **77**, 639 (2000).

[24] Y. M. Niquet, C. Delerue, G. Allan, and M. Lannoo, Phys. Rev. B **65**, 165334 (2002).

[25] C. Delerue, G. Allan, and Y. M. Niquet, Phys. Rev. B **72**, 195316 (2005).

[26] E. Martin, C. Delerue, G. Allan, and M. Lannoo, Phys. Rev. B **50**, 18258 (1994).

[27] M. Lannoo, C. Delerue, and G. Allan, Phys. Rev. Lett. **74**, 3415 (1995); C. Delerue, M. Lannoo, and G. Allan, Phys. Rev. B **56**, 15306 (1997).

[28] We have checked that it is fully justified by the numerical calculation of Γ.

[29] D. L. Dexter, in *Solid State Physics, Advances in Research and Applications*, edited by F. Seitz and D. Turnbull (Academic, New York, 1968), Vol. 6, p. 360.

[30] C. Delerue, M. Lannoo, and G. Allan, Phys. Rev. B **68**, 115411 (2003).

[31] X. Cartoixà and L.-W. Wang, Phys. Rev. Lett. **94**, 236804 (2005).

[32] L. W. Wang and A. Zunger, Phys. Rev. Lett. **73**, 1039 (1994).

[33] In Refs. 27 and 30, we used a different expression for the size dependence of the average dielectric constant. However, we have realized that Eq. (15) is simpler and more physical, and it still provides a very good fit of the average dielectric constant calculated in Ref. 30.

[34] C. J. F. Böttcher, *Theory of Electric Polarization*, 2nd ed. (Elsevier, Amsterdam, 1973), Vol. 1.

[35] M. S. Hybertsen, Phys. Rev. Lett. **72**, 1514 (1994).

[36] C. Delerue, G. Allan, and M. Lannoo, Phys. Rev. B **64**, 193402 (2001).

[37] L. Hedin and S. Lundqvist, *Solid State Physics*, edited by H. Ehrenreich, F. Seitz, and D. Turnbull (Academic, New York, 1969), Vol. 23.